

Effect of the pH and heat on the stability and spectral properties of mercury (II) and copper (II) azo complexes

Hasanain A. Abdullmajeed^{1*}, Ihsan A. Alasady¹, Hadi T. Obaid², Jassim H. Al-Waeli³, Ghufraan A. Mirdan⁴

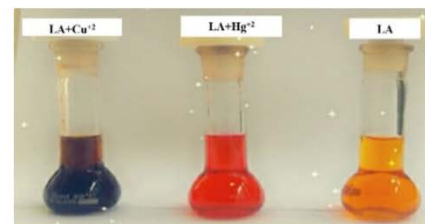
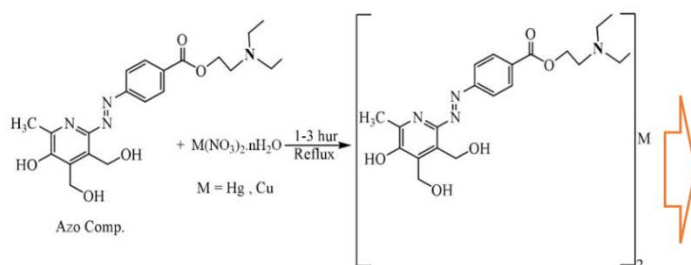
¹Department of Chemistry, College of Education for Pure Sciences, University of Basrah, Basrah 61007, Iraq. ²Department of English, College of Education, University of Shatrah, Thi-Qar 64002, Iraq. ³General Directorate of Education in Thi-Qar, Ministry of Education, Thi-Qar 64002, Iraq. ⁴General Directorate of Education in Basrah, Ministry of Education, Basrah 61007, Iraq.

Submitted on: 16-Jul-2025, Revised: 12-Sep-2025, Accepted and Published on: 15-Sep-2025

Article

ABSTRACT

This study focuses on the preparation of complexes of mercury(II) and copper(II) with an azo ligand (LA). The metal complexes were



characterized using infrared spectroscopy, flame atomic absorption, magnetic susceptibility measurements, continuous change, and thermal analysis. The complexes have a four-coordination geometric shape and were studied using a spectrum method. The acid function effect was measured using solutions with an acid function range (2–12) and the maximum wavelength for the mercury (II) and copper (II) complexes (520 and 480 nm) at pH 5 and 12. The study also investigated Beer's law applied to the azo molecule (LA) and the spectroscopic method's sensitivity to these complexes. The findings indicate that the complexes exhibit notable differences in their spectral responses across varying pH levels. Furthermore, the data suggest that the azo molecule's interaction with the metal ions enhances its applicability in analytical chemistry, particularly in environmental monitoring and industrial applications. The results are crucial for developing industrial and medical applications.

Keywords: Metal complexes, Acid-Base Properties, Thermal analysis, Beer's law

INTRODUCTION

Color chemistry is mostly about azo ligands, which are man-made azo ligands with the (-N=N-) part. William Henry Perkin is thought to have started the synthetic azo ligand business when he found mauveine, a purple azo ligand, by mistake in 1856.^{1,2}

Later, Peter Griess's work paved the way for the growth of azo ligands and pigments chemistry, which in turn led to the most important color chemistry finding in 1858.³⁻⁵ Azo ligands come in different colors like yellow, red, and orange. Azo ligands have been used to add color to many products such as clothes, paper, food, cosmetics, drugs, and more.⁶ TG and DTA are extensively utilized in material characterization.⁷ These techniques fundamentally rely

on measuring alterations in physical-chemical properties in relation to increase the temperature over time.⁸⁻¹⁰ Metal (II) azo complexes exhibit vibrant colors and are extensively utilized as azo ligands and pigments in various applications, including textile dyeing, nonlinear optics, and photoelectronic, particularly in optical information.¹¹⁻¹⁵ The aim of this study is to study the spectral and thermal properties of complexes of azo ligand (LA) with copper (II) and mercury (II), given the importance of knowing the stability of complexes prepared from azo ligand (LA), which has multiple industrial and medical uses.

MATERIALS AND METHODS

In the characterization methods, utilized a JASCO/Japan FT-IR 4200 with sodium bromide plates in the infrared range. Temperatures by melt science [9100]. The visible spectrum was tracked by the JENWAY [6305] Spectrophotometer. A precise scale and an Oakion pH 2100 Series pH meter was used to get the target results. The HI 2315 conductivity Meter to measure the molar conductivity of the mixtures in DMF. A Msb-Mki Balance Magnetic Susceptibility Modifier was used to measure the

*Corresponding Author: Hasanain A. Abdullmajeed, Department of Chemistry, College of Education for Pure Sciences, University of Basrah, Basrah 61007, Iraq. Tel: +964 771 739 5407; Email: hasanain.abdullmajeed@uobasrah.edu.iq

Cite as: J. Integr. Sci. Technol., 2025, 13(8), 1177.
URN: NBN:sciencein.jist.2025.v13.1177
DOI: 10.62110/sciencein.jist.2025.v13.1177



complexes' magnetic susceptibility at 25°C. The temperature range of 25 to 1000 °C and a heating rate of 10 °C.min⁻¹ in an argon-filled room were used.

2.1 Preparation of mercury complex

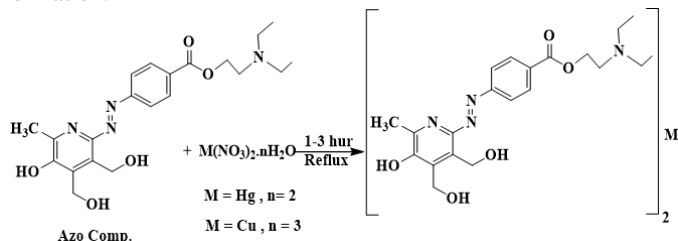
A 100 ml round flask should have 0.3607 g (0.001 mole) of mercury (II) nitrate trihydrate mixed with 20 ml of absolute ethanol and 0.8330 g (0.002 mole) of azo ligand (LA) mixed with 30 ml absolute ethanol, and refluxing for three hours. Cooling the mixture got rid of the parts that hadn't reacted yet. The crystals that had formed were then filtered and washed with water, hot ethanol, and ether. The yield was 59%, the melting point was 300 °C, and the FTIR lines were 3298 (ν O-H), 1440 (ν N=N), and 1287 (ν C-N). The metal to ligand ratio was 1:2, the molar conductivity was 4.1 Ohm⁻¹.cm².mol⁻¹, the magnetic susceptibility was 0, and the hybridization was sp³.¹⁶

2.2 Preparation of copper complex

A round jar that holds 100 ml of absolute ethanol and 0.2416 g (0.001 mole) of copper (II) nitrate trihydrate mixed with 20 ml absolute ethanol. 0.8330 g (0.002 mole) of azo ligand (LA) mixed with 30 ml absolute ethanol, and refluxes for an hour. It was filtered and washed with water, hot ethanol, and ether to get rid of the parts that didn't respond after the mixture cooled. A 64% return on the brown crystals. The melting point was between 182 and 187 °C, the metal to ligand ratio was 1:2, the molar conductivity was 6.4 Ohm⁻¹.cm².mol⁻¹, and the magnetic susceptibility was 1.98, it could have been sp³ or dsp².¹⁷ The complexes [Hg(LA)₂, Cu(LA)₂] were schematically showed in Scheme 1.

2.3 Visible absorption spectrum of the complexes Hg(LA)₂ and Cu(LA)₂ in solutions of different pH values

We made several protective solutions by mixing a universal buffer solution with a range of pH values (2–12) and adding different amounts of Hg(LA)₂ and Cu(LA)₂ complexes at a concentration of 8×10⁻⁵ M for LA. The pH value over a range of wavelengths, from 350 to 570 nm, and examine these solutions formation.



Scheme 1. Synthesis of complexes Hg(LA)₂ and Cu(LA)₂.

RESULTS AND DISCUSSION

3.1 Identification of the prepared complexes Hg(LA)₂ and Cu(LA)₂.

The spectra of complex complexes Hg(LA)₂ and Cu(LA)₂ exhibit bands (3298 and 3253 cm⁻¹) respectively due to the ν(O-H) group. The azo ligand of the frequency of the azo group ν(N=N) towards lower or higher frequency regions with a noticeable change in its shape and intensity in the spectral range (1440 and 1406 cm⁻¹), respectively. It was also observed in the spectra of the complexes that weak nine-frequency bands at the frequency (530

and 524 cm⁻¹) respectively belong to the ν(N-O) bond¹⁸⁻²⁰ as presented in Figures 1a and 1b.

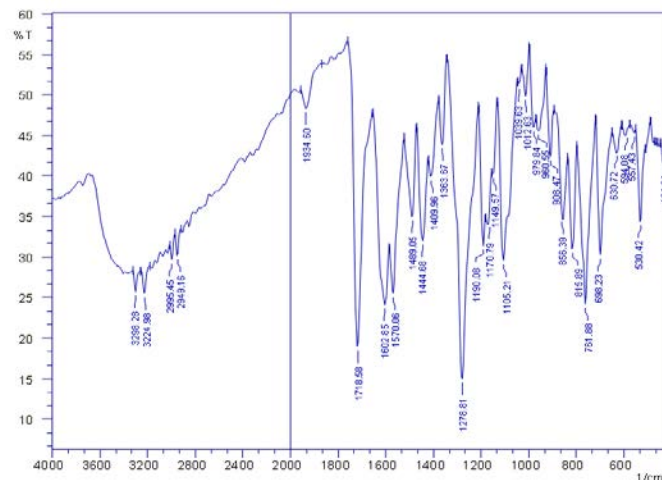


Figure 1a. Infrared spectrum of the complex Hg(LA)₂.

3.2 Estimation of the percentage of copper (II) in the complex

Flame atomic absorption spectroscopy (AAS) was used to estimate the ratio of the metal to the azo ligand in the Hg(LA)₂ and Cu(LA)₂ complexes. This procedure involves diluting the sample with ion-free distilled water and then entering the flame atomic absorption device for measurement.²¹ It is observed the values and calculations of the practical percentages are very close to the values and calculations of the theoretical percentages, which calculated for the metals involved in the composition of the complexes. The results confirm that the ratio of metal to azo ligand in this complex is 1:2 (Metal: Ligand), as shown in Table 1.

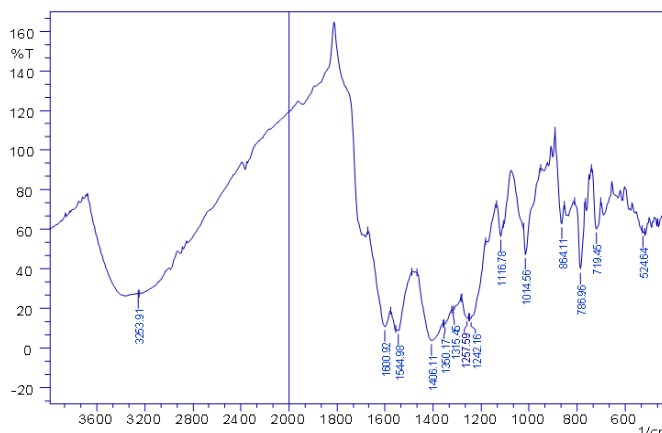


Figure 1b. Infrared spectrum of the complex Cu(LA)₂.

Table 1. Proportions of copper(II) in its complex using flame atomic absorption technology.

[Cu] in (AAS) g x10 ⁻⁶	Molecular weight g.mol ⁻¹	Weight g	Comple x	Cu (II)%		M: L
				Theoretic al	Practic al	
1090	894.49	0.0106	Cu(LA) ₂	8.90	9.10	1 : 2

3.3 Molar electrical conductivity

The molar conductivity of solutions of copper (II) complexes was measured in dimethylformamide (DMF) solvent with a concentration of (1×10^{-3} M) at room temperature, by using the equations (1 and 2)²²:

$$L = G \times A \dots\dots 1$$

$$\Lambda_M = 1000 \times L / C \dots\dots 2.$$

We noticed from the molar conductivity values listed in Table 2, that $\text{Hg}(\text{LA})_2$ and $\text{Cu}(\text{LA})_2$ complexes were low, as the molar conductivity value ranged between (4.1 and $6.4 \text{ Ohm}^{-1} \cdot \text{cm}^2 \cdot \text{mol}^{-1}$), respectively. The lack of ionic character indicates the absence of negative ions outside the coordination ball for all complexes.²³

Table 2. Values of electrical conductivity, molarity, and electrolyte for complexes $\text{Hg}(\text{LA})_2$ and $\text{Cu}(\text{LA})_2$.

Type of electrolyte	Molar conductivity $\text{Ohm}^{-1} \cdot \text{cm}^2 \cdot \text{mol}^{-1}$	Electrical conductivity $\text{S} \times 10^{-6}$	Complex
Non-electrolytic	4.1	3.7	$\text{Hg}(\text{LA})_2$
Non-electrolytic	6.4	5.8	$\text{Cu}(\text{LA})_2$

3.4 Magnetic susceptibility measurements

The results of the magnetic susceptibility technique measurements reinforce that the predict of the proposed stereo forms of the studied complexes and reinforce with other diagnostic techniques have reached about structure and stereoscopic shape²⁴. Additional information can also be obtained about the oxidation state of the central atom in the complex and the electronic arrangement²⁵. Through the experimental values of the effective magnetic moment (μ_{eff}), we can determine whether the central atom possesses one or more single electrons, which will show the complex with paramagnetic properties, or if it does not have a single electron, which will lead to the appearance of magnetic properties.^{26,27}

The experimental values of the effective magnetic moment (μ_{eff}) of the studied metal complexes were calculated at room temperature (298 K), and the diamagnetic correction of the atoms in organic molecules, inorganic radicals, and metal ions was carried out using Pascal's constants²⁸ according to the following equations:

$$\mu_{\text{eff}} = 2.828 \sqrt{X_A T} \dots\dots 3$$

$$X_A = X_M - D \dots\dots 4$$

$$X_M = X_g \times M. \text{wt} \dots\dots 5$$

$$X_g = [C \times L / 109 \text{ m}] \times (R - R^\circ) \dots\dots 6$$

The magnetic susceptibility results shown in the Table 3 confirm that the mercury(II) complex with the azo ligand (LA) exhibited diamagnetic properties, confirming the electronic configuration of mercury (II) $[\text{Xe}] 4f^{14} 5d^{10} 6s^0$. The complex's geometry is tetrahedral with sp^3 hybridization. The copper (II) complex with the azo ligand (LA) was found to exhibit paramagnetic properties due to the presence of only one electron, confirming the electronic configuration of copper (II) $[\text{Ar}] 3d^9 4s^0$. The expected geometry of the copper(II) complex is tetracoordinated, which is either a tetrahedral with sp^3 hybridization or a planar square with dsp^2 crystallization.

Table 3. Magnetic susceptibility data for $\text{Hg}(\text{LA})_2$ and $\text{Cu}(\text{LA})_2$ complexes.

Comple x	-D 10^{-6}	X_g 10^{-6}	X_M 10^{-6}	X_A 10^{-6}	μ_{eff}	Hybridizati on
$\text{Hg}(\text{LA})_2$	540.4 4	0	0	0	0	sp^3
$\text{Cu}(\text{LA})_2$	520.2 4	1.2 5	1118.1 4	1638.3 8	1.9 8	sp^3 or dsp^2

3.5 Thermogravimetric analysis

Thermal analyses are important measurements in studying the stability and composition of coordination complexes, through which the water molecules bound in the form of a water lattice can be identified. A study indicates that the water bound to the crystal is often lost in the first stage of heating, at temperatures between approximately (30 and 150°C).²⁹ For the water molecules linked by coordination to the central atom, they separate from the coordination complex in the second stage, at a higher temperature range than the water molecules of crystallization. In the literatures indicate that the temperatures range between (120 and 220°C).³⁰ For the subsequent stages, they include the dissociation of the negative ions bound to the central atom, then the stages of dissociation of the ligand, and finally the metal oxides that are part of the complexes, which remain at high temperatures. We noted from the thermogravimetric analysis curves of the mercury (II) and copper (II) complexes with azo ligand (LA), that the "lost part" consists of several stages, as shown in Figures 2a and 2b. The mercury (II) complex with azo ligand (LA) consists of three stages, while the copper (II) complex with azo ligand (LA) consists of two stages. The thermal analysis stages involve the loss of all or parts of the complex's ligand, corresponding to the weight lost within the temperature range of (200 - 800°C). The "remaining part", which includes the thermal analysis products visible in all of these curves, is the mercury (II) or copper (II) metals, in the form of mercury (II) oxide (HgO) or copper(II) oxide (CuO), respectively, at temperatures above 1000°C .

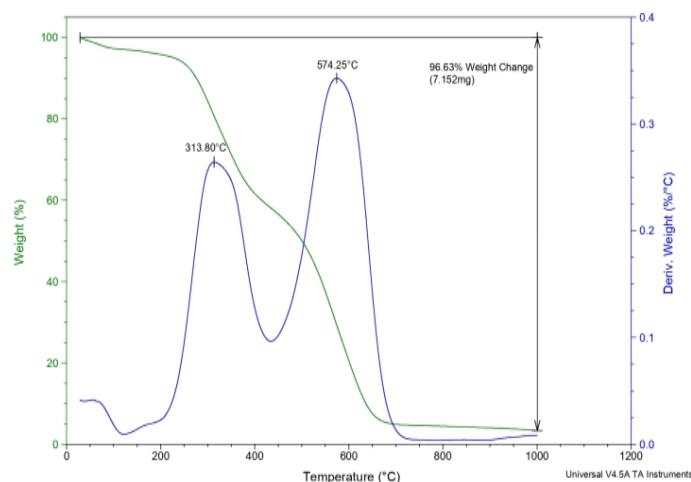


Figure 2a. Thermal analysis curve of the complex $\text{Hg}(\text{LA})_2$.

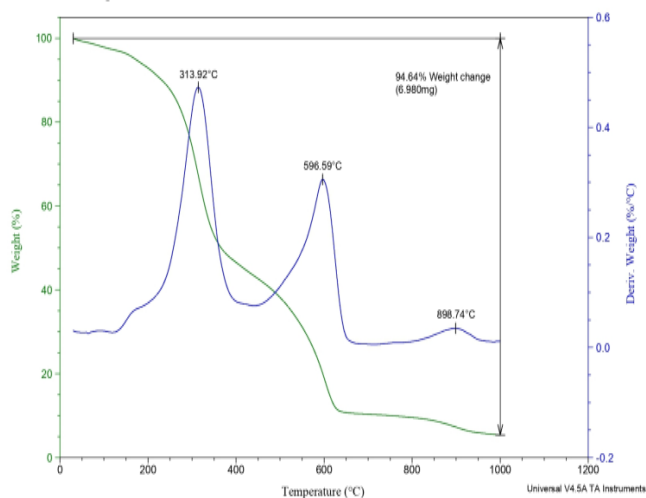


Figure 2b. Thermal analysis curve of the complex $\text{Cu}(\text{LA})_2$.

3.6 Optimal conditions for the formation of azo complexes

We studied the optimum conditions for forming mercury (II) and copper (II) complexes with the azo ligand (LA) at room temperature. This step is essential for conducting subsequent spectroscopic studies on the two complexes. We noted the color change of the azo ligand (LA) from orange to red and walnut with the mercury (II) and copper (II) ions, respectively. This variation is preliminary evidence for the formation of the two complexes, as shown in Figure 3.

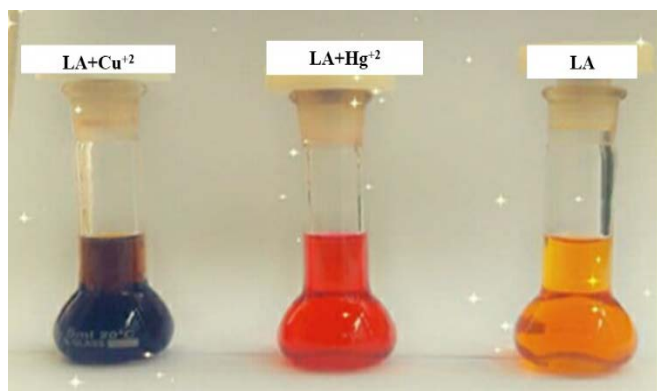


Figure 3. Change in color of azo ligand (LA) when it complexes with mercury (II) and copper (II) ions.

3.7 Effect of acidity function

The absorption spectra of solutions of mercury (II) and copper (II) ionic complexes, respectively, with the azo ligand (LA), were studied using buffer solutions (collector buffer solutions) with a pH range of (2-12). Absorption was measured in the visible region over a wavelength range (350-570 nm), using the ligand solution and the buffer solution as references. The spectra of the mercury (II) complex with the azo ligand (LA) show two peaks: the first at (430 nm) at pH between 9 and 12, and a second peak showing the highest absorption at the maximum wavelength between (460 and 520 nm) at pH between 2 and 8, as shown in Figure 4a. In the spectra of the copper (II) complex with the azo ligand (LA), two peaks are

observed: the first at (470 nm) at pH values between 2 and 7, and the second peak shows the highest absorption at the maximum wavelength (490 nm) at pH values between 8 and 12, respectively, as shown in Figure 4b. The acidity plays a significant role in increasing the efficiency of the active groups in the azo ligand for optimal and stronger bonding with the metal ion to form the complex, which has the highest formation constant at the optimum pH. Therefore, a buffer solution with a pH 5 is suitable for the mercury (II) complex with azo ligand (LA) at a maximum wavelength of (520 nm), while a pH 12 for the copper (II) complex with azo ligand (LA) at a maximum wavelength of (480 nm) is more suitable for complex formation.

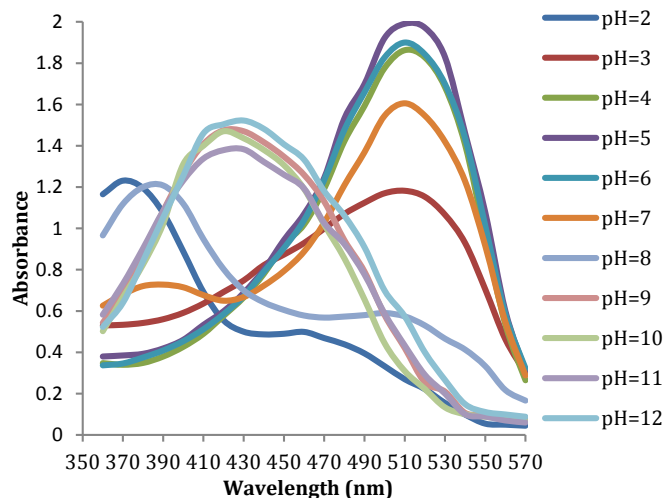


Figure 4a. Visible absorption spectrum of the mercury (II) complex with the azo ligand (LA) in buffer solutions of different pH, $[\text{LA}] = [\text{Hg}^{+2}] = 8 \times 10^{-5} \text{ M}$.

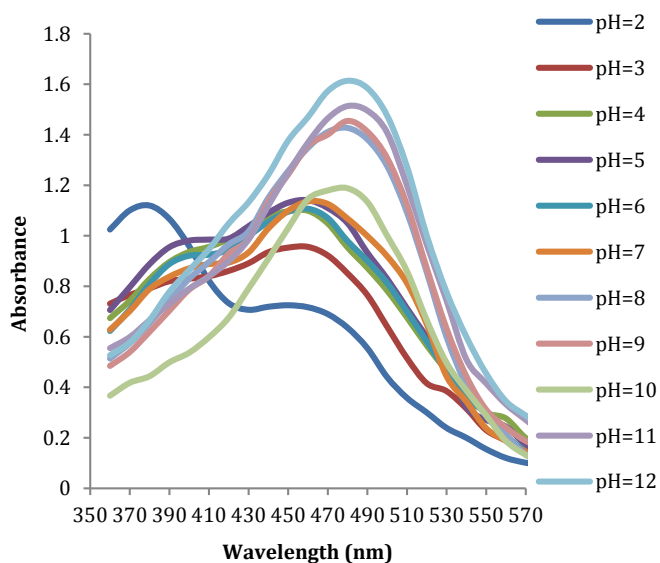


Figure 4b. Visible absorption spectrum of copper (II) complex with azo ligand (LA) in buffer solutions of different pH, $[\text{LA}] = [\text{Cu}^{+2}] = 8 \times 10^{-5} \text{ M}$.

3.8 Kinds of buffer solution of pH 5 and 12

To assess the influence of different buffer solutions on attaining the maximum absorbance of the mercury (II) complex with the azo ligand (LA) at pH 5, numerous buffer solutions were formulated to sustain this pH (1 =Universal, 2 =Hexamine, 3 = $\text{H}_3\text{BO}_3+\text{NaOH}$, 4 = $\text{KHC}_8\text{H}_4\text{O}_4+\text{NaOH}$, 5 = $\text{KH}_2\text{PO}_4+\text{NaOH}$), as shown in Figure 5a. A genuine buffer solution with a pH of 5 consists of KH_2PO_4 and NaOH . To evaluate the influence of various buffer solutions on achieving the maximum absorbance of the copper (II) complex with azo ligand (LA) at pH 12.

Several buffer solutions were formulated to get this pH level: 1=Universal, 2=Hexamine, 3=[$\text{H}_3\text{BO}_3+\text{NaOH}$]+ NaOH , 4= $\text{KCl}+\text{NaOH}$, 5= $\text{Na}_2\text{HPO}_4.2\text{H}_2\text{O}+\text{NaOH}$. A genuine buffer solution with a pH of 12 consists of $\text{Na}_2\text{HPO}_4.2\text{H}_2\text{O}$ and NaOH , as shown in Figure 5b.

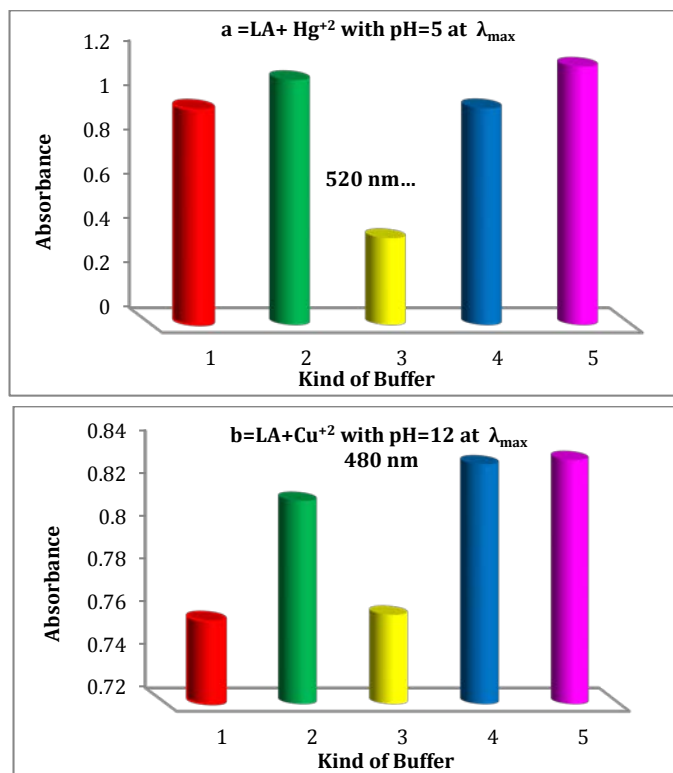


Figure 5. Absorption of complexes ($\text{LA}+\text{Hg}^{2+}$) and ($\text{LA}+\text{Cu}^{2+}$) at a concentration of (4×10^{-5} M) in different buffer solutions at pH 5 and 12 respectively.

3.9 Selection of maximum wavelength (λ_{max})

Choosing the maximum wavelength is one of the most important considerations when studying the optimum conditions for complex formation. The study was conducted in the visible spectrum (350-570 nm) for the azo ligand (LA) and its complex with mercury (II) and copper (II) ions. The maximum wavelengths of the azo ligand (LA) and its complex with the mercury (II) ion were found to be (480 and 520 nm), respectively, in ethanol solvent and (380 and 510 nm), respectively, in acidic buffer solution pH 5, as shown in Figure 6a. The maximum wavelengths of the azo ligand (LA) and its complex with copper (II) were found to be (480 and 500 nm),

respectively, in ethanol solvent and (430 and 480 nm), respectively, in acidic buffer solution pH 12. The large difference in maximum wavelengths and the shift towards a higher wavelength of the complexes with the azo ligand are evidence and confirmation of the formation of these complexes, as shown in Figure 6b.

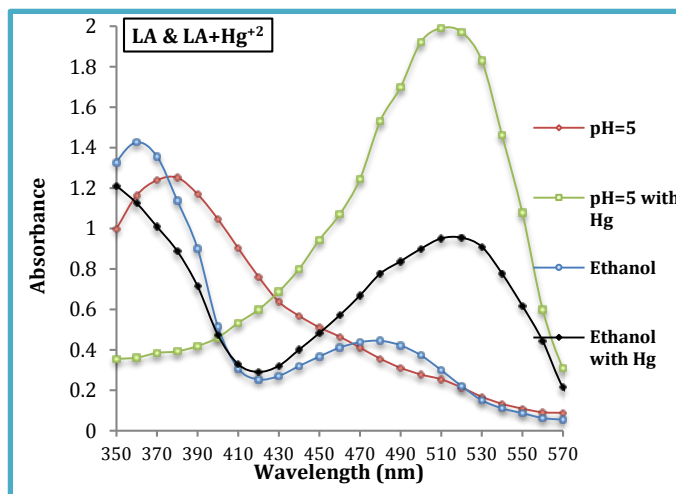


Figure 6a. Visible absorption spectrum of the azo ligand (LA) and its complex with mercury(II) using a solution (ethanol, pH 5) as a reference, respectively, $[\text{LA}]=[\text{Hg}^{2+}]=8 \times 10^{-5}$ M.

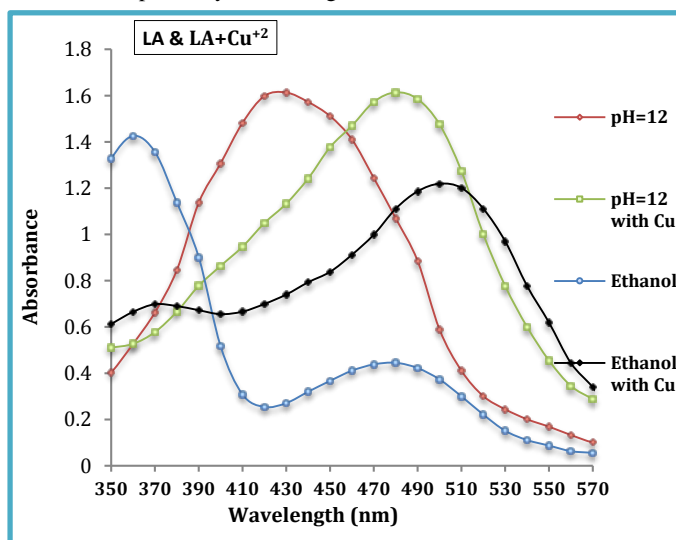


Figure 6b. Visible absorption spectrum of the azo ligand (LA) and its complex with copper (II) using a solution (ethanol, pH 12) as a reference, respectively, $[\text{LA}]=[\text{Cu}^{2+}]=8 \times 10^{-5}$ M.

3.10 The effect of time

The time changed from 1 to 2880 minutes to observe the spectrum of mercury (II) and copper (II) ion complexes with the azo ligand (LA). The longest range for the mercury (II) ion complex with the azo ligand (LA) was 520 nm. A buffer solution with a pH of 5 was used as a standard. The absorption spectrum of the copper (II) ion complex with the azo ligand (LA) at a wavelength of 480 nm, using a pH 12 buffer solution as a standard was followed and observed. The results showed that the combinations stay stable for up to 2880 minutes, as shown in Figure 7 and Table 4.

Table 4. Effect of time on the breakdown patterns of mercury (II) and copper (II) complexes with azo ligand (LA).

Time (min)	Absorbance LA+Hg ²⁺ at λ_{max} 520 nm	Absorbance LA+Cu ²⁺ at λ_{max} 480 nm
1	1.989	1.655
5	1.981	1.657
10	1.984	1.660
15	1.990	1.664
20	1.991	1.667
25	1.988	1.665
30	1.987	1.669
40	1.985	1.673
50	1.983	1.677
60	1.985	1.666
120	1.993	1.675
180	1.990	1.672
1440	1.995	1.670
2880	1.993	1.666

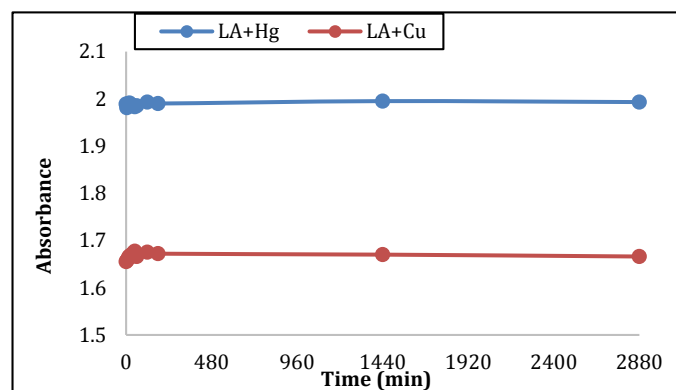


Figure 7. Effect of time on the absorption of mercury(II) and copper(II) complexes with azo ligand a solution (pH 5 and 12) as a reference, respectively, $[LA]=[Hg^{2+}]=[Cu^{2+}]=8 \times 10^{-5}$ M.

3.11 Effect of successive addition

The results obtained from three different addition sequences indicate that the addition sequence (LA + pH + Metal) is the most suitable for the mercury (II) complex with the azo ligand (LA). The addition sequence (LA + Metal + pH) was found to be the most suitable for the copper (II) complex with the azo ligand (LA). Due to the formation of a direct stable complex between the mercury (II) and copper (II) ions with the respective azo ligand. Table 5, shows the absorption values at the maximum wavelength.

Table 5. Effect of addition sequence on the absorption values of mercury (II) and copper (II) complexes with azo ligand (LA).

Addition sequence	Absorbance LA+Hg ²⁺ at λ_{max} 520 nm	Absorbance LA+Cu ²⁺ at λ_{max} 480 nm
LA + Metal + pH	1.877	1.663
LA + pH + Metal	1.991	1.579
Metal + pH + LA	1.817	1.361

Table 6. Absorbance values of mercury (II) and copper (II) complexes with azo ligand (AL) at λ_{max} to calculate the molecular structure by the continuous variation method.

[LA] $\times 10^{-4}$ M	[M ²⁺] $\times 10^{-4}$ M	[M ²⁺]/([M ²⁺] + [LA])	Absorbance LA+Hg ²⁺ at λ_{max} 520 nm	Absorbance LA+Cu ²⁺ at λ_{max} 480 nm
1.9	0.1	0.05	1.009	0.796
1.8	0.2	0.1	1.152	0.897
1.6	0.4	0.2	1.400	1.070
1.4	0.6	0.3	1.821	1.100
1.2	0.8	0.4	1.696	1.066
1.0	1.0	0.5	1.757	1.087
0.8	1.2	0.6	1.444	1.004
0.6	1.4	0.7	1.195	0.888
0.4	1.6	0.8	0.839	0.799
0.2	1.8	0.9	0.720	0.669

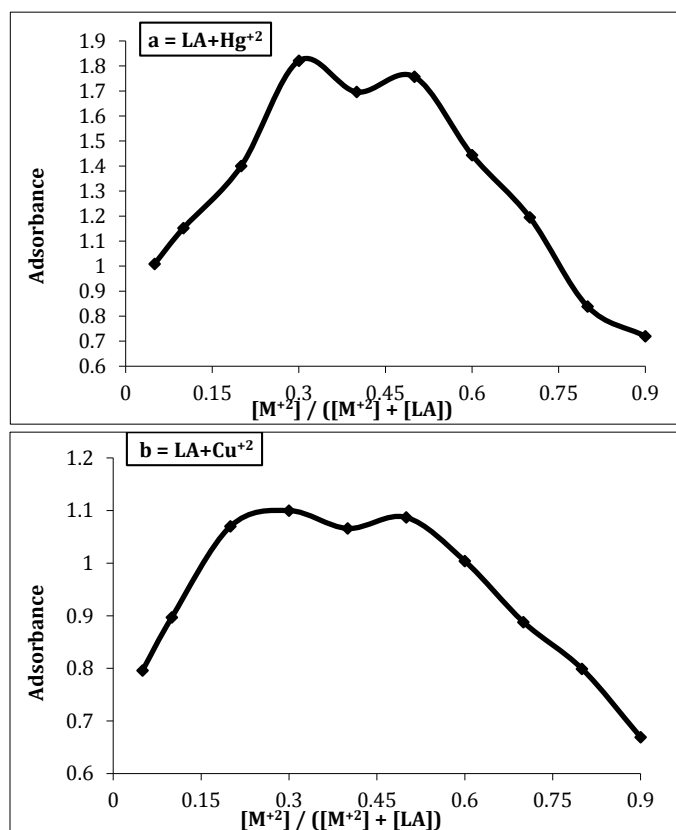


Figure 8. Molecular structures of mercury (II) and copper (II) complexes respectively with the azo ligand (LA) at λ_{max} .

3.12 Determination the molecular ratios of mercury(II) and copper(II) ionic complexes by Job's method

The absorption values of the mercury (II) and copper (II) ion complexes with the azo ligand (LA) were plotted, respectively, against the molar fraction of the metal, as shown in Table 6 and Figure (8a and 8b). It is noted that two peaks appear at (0.33) and (0.5), which indicates the formation of a stepwise (intermediate) (ML) complex and the formation of a final (ML₂) complex.

3.13 Calculate the formation constants (stability constants) of the mercury(II) and copper(II) complexes with the azo ligand (LA)

To verify and determine the stability of mercury(II) and copper(II) complexes with the azo ligand (LA), the stability constants of these complexes were calculated spectroscopically from the information obtained from the continuous variation method and by applying the special equations for calculating constants³¹:

$$K_1 = (1-\alpha)/(\alpha^2 c); \text{ for } 1:1 \text{ (LA:M) } \dots\dots 7$$

$$K_2 = (1-\alpha)/(4\alpha^3 c^2); \text{ for } 2:1 \text{ (LA:M) } \dots\dots 8$$

Where α represents the degree of dissociation and c represents the molar salt concentration of the metal. The value of α can be calculated from the equation:

$$\alpha = (A_m - A_s)/A_m \dots\dots 9$$

Table 7. Values of (A_m , A_s , α , c , K_1 and K_2) for the complexes of mercury (II) and copper (II) with the azo ligand (LA).

LA with	[M ⁺²] ×10 ⁻⁵ M	A _m	A _s	α	K ₁ ×10 ⁶	K ₂ ×10 ¹¹
Hg ⁺²	8	1.100	1.087	0.020	30.6	47.80
Cu ⁺²	8	1.821	1.757	0.035	9.85	8.79

The absorption in the presence of an excess of the chelating agent azo ligand (LA) is represented by A_m , while the absorption at equal amounts of both the metal and the chelating agent is represented by A_s . Table 7, shows the values of A_m , A_s , α , c , K_1 , and K_2 for the complexes. The values for the complexes of mercury (II) and copper (II) with the azo ligand (LA) are shown in Table 7, which also indicates that the mercury complex (LA+Hg⁺²) is more stable than the copper complex (LA+Cu⁺²).

3.14 Beer's Law and Method Sensitivity

The spectrophotometric determination of mercury (II) and copper (II) ions involved an investigation of Beer's law applicability to their complex solutions, utilizing a calibration curve that correlates absorbance values with concentrations in parts per million (ppm), as illustrated in Figure 9a and 9b. The method's sensitivity is often indicated by the slope of the calibration curve. This term often refers to the lowest quantifiable concentration of the species, determined by the molar absorption coefficient (ϵ) at the peak wavelength of the complex. The outcome is a numerical representation of the method's sensitivity, equivalent to the slope of the calibration curve plotted between absorbance values and molar concentrations, in accordance with Beer's law.³² The curve's slope and the correlation coefficient (r) are computed directly by a computer, respectively.

Table 8, shows the specific absorptivity (LA) values, which represent the absorbance of a solution at a concentration of (1 $\mu\text{g}.\text{ml}^{-1}$) in a cell with an optical path length of 1 cm. This quantity is an important factor in determining the sensitivity of the method and is determined in terms of the molar absorption coefficient, as in the equation:

$$a = \epsilon / \text{At.wt} \times 1000 \dots\dots 10 \text{ (At.wt represents the atomic weight of the metal).}$$

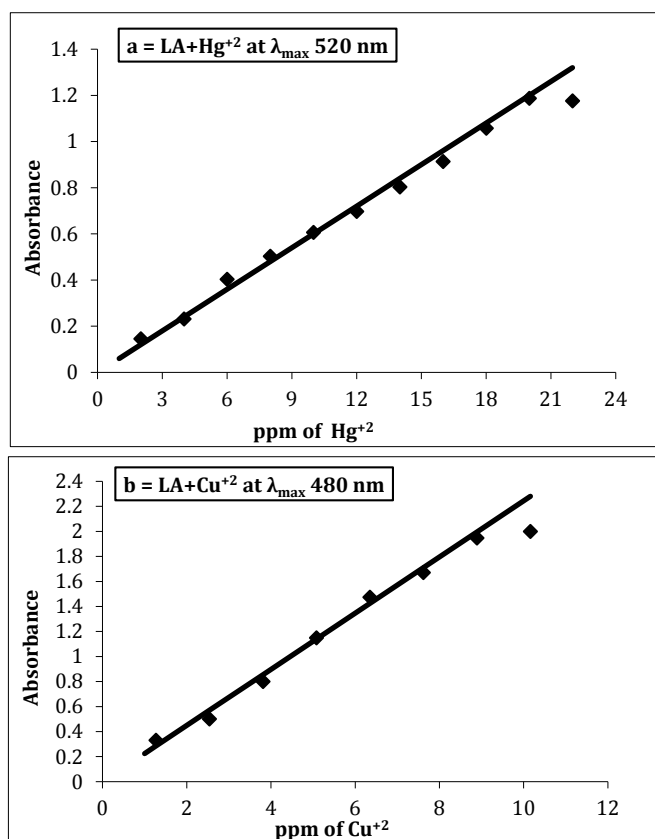


Figure 9. Determination curve (Beer's law) of mercury(II) and copper(II) complexes with azo ligand (LA) at λ_{max} .

Table 8. Results obtained from Beer's law for the complexes of mercury(II) and copper(II) respectively with the azo ligand (LA) at λ_{max} .

LA with	λ_{max} nm	ppm	$\epsilon \times 10^4$ L. mol ⁻¹ . cm ⁻¹	a ml. g ⁻¹ . cm ⁻¹	R ²	S $\mu\text{g}.\text{cm}^{-2}$	S.D	DL $\mu\text{g}.\text{ml}^{-1}$
Hg ⁺²	520	22.00	2.49	0.124	0.991	0.008	0.005	0.40
Cu ⁺²	480	8.89	2.09	0.329	0.988	0.003	0.009	0.86

$$\text{At. wt (Hg and Cu)} = (200.59 \text{ and } 63.55 \text{ g.mol}^{-1}) \text{ respectively.}$$

Table 8, also shows the Sandell sensitivity (S) value,³³ which is another expression for the sensitivity of the spectroscopic method and represents the number of micrograms of the substance to be determined per milliliter of solution with an absorbance value of (0.001) in a cell with an optical path length of (1 cm). In this case, the sensitivity is expressed in units of $\mu\text{g}.\text{cm}^{-2}$, and the Sandell sensitivity is expressed in terms of specific absorptivity according to equation:

$$S = 10^{-3}/a \dots\dots 11$$

The standard deviation (S.D) of six readings is used to demonstrate how closely the calculated readings agree with each

other, and it also helps determine the detection limit (DL) using the equation

$$DL = 2 S.D \times \text{Concentration of Metal} / \text{Mean of Abs} \dots 12$$

CONCLUSIONS

The results of spectroscopic studies and thermogravimetric analysis of the mercury (II) and copper (II) with azo ligand (LA) showed the formation of complexes. The Beer's law, high linearity and sensitivity of the method for the determination of mercury (II) and copper (II) using azo compound (LA) solutions at their maximum wavelengths were demonstrated. Also, the sensitivity of the method was confirmed by calculating the molar absorption coefficient, specific absorptivity, correlation coefficient, detection limits, Sandell sensitivity, upper limits of Beer's law and standard deviation. It is easy, sensitive, fast and has high accuracy and precision. The importance of knowing the stability of the complexes utilized for the industrial and medical in the future uses.

CONTRIBUTION STATEMENT

Planning, analysis, and writing of the manuscript: HAA and GAM; Synthesis and analysis experiments: HTO, JHW, and IAA; The final form of the manuscript was agreed upon by all authors.

ACKNOWLEDGMENT

This research is supported by the Chemistry Department, College of Education for Pure Sciences, University of Basrah, Iraq.

REFERENCES

1. S. Benkhaya, S. M' rabet, A. El Harfi. A review on classifications, recent synthesis and applications of textile dyes. *Inorganic Chem. Commun.* **2020**, 115, 107891.
2. J.H. Al-Waeli, H.A. AbdullMajed, S.M. Ismael. Studies of spectroanalytical and the biological effectiveness of the Azo compound (J25) prepared from Ethyl p-aminobenzoate. *Basrah Researches Sciences* **2024**, 50 (1), 11.
3. R. Khanum, R.A. Shoukat Ali, H.R. Rangaswamy, et al. Recent review on Synthesis, spectral Studies, versatile applications of azo dyes and its metal complexes. *Results in Chemistry* **2023**, 5 (March), 100890.
4. J.H. Al-Waeli, H.A. Abdull-Majed, M.A. Ibrahim, S.M.H. Ismael. Synthesis of a Novel Chemical J5 brown Dye for Staining Specific Bone Histological Sections in Green Swordtail Fish (*Xiphophorus hellerii*). *Trop. J. Nat. Prod. Res.* **2025**, 9 (3), 1025–1030.
5. R.M. Christie. Colour: A brief historical perspective. *Colour Chemistry* **2007**, 1–11.
6. F. Eltaboni, N. Bader, R. El-Kailany, N. Elsharif, A. Ahmida. Chemistry and Applications of Azo Dyes: A Comprehensive Review. *J. Chem. Rev.* **2022**, 4 (4), 313–330.
7. P. Belina, P. Sulcova. Utilization of DTA for two-step synthesis of Cu – Mn – Cr spinel. *Journal of thermal analysis and calorimetry*, **2007**, 88, 107–110.
8. C. Leyva-Porras, P. Cruz-Alcantar, V. Espinosa-Sol, M.Z. Saavedra-Leos. Application of Differential Scanning Calorimetry (DSC) and Modulated Differential Scanning. *Polymers* **2019**, 12 (5), 1–21.
9. Broido A. Simple, Sensitive Graphical Method of Treating Thermogravimetric Analysis Data. *J Polym Sci Part A-2 Polym Phys* **1969**, 7 (10), 1761–1773.
10. M.M. Aftan, A.A. Talloh, A.H. Dalaf, H.K. Salih. Impact para position on rho value and rate constant and study of liquid crystalline behavior of azo compounds. *Materials Today: Proceedings* **2021**, 45 (xxxx), 5529–5534.
11. S. Wang, S. Shen, H. Xu. Synthesis, spectroscopic and thermal properties of a series of azo metal chelate dyes. *Dyes and Pigments* **2000**, 44 (3), 195–198.
12. X.Y. Li, Y.Q. Wu, D.D. Gu, F.X. Gan. Optical characterization and blu-ray recording properties of metal(II) azo barbituric acid complex films. *Materials Science and Engineering: B* **2009**, 158 (1–3), 53–57.
13. H.E. Katz, K.D. Singer, J.E. Sohn, et al. Greatly Enhanced Second-order Nonlinear Optical Susceptibilities in Donor—Acceptor Organic Molecules. *J. Am. Chem. Soc.* **1987**, 109 (21), 6561–6563.
14. F. Gan, L. Hou, G. Wang, H. Liu, J. Li. Optical and recording properties of short wavelength optical storage materials. *Mater. Sci. Engin.: B* **2000**, 76 (1), 63–68.
15. H.A. Abdullmajed, A.A. Ali, R.H. AL-Asadi. Preparation and Spectroanalytical Studies of Two New Azo Compounds Derived from the Drug Methyl-4-Amino Benzoate. *AIP Conference Proceedings* **2023**, 2457 (February).
16. H.A. Abdullmajed, I.A. Alasady, H.T. Obaid, G.A. Mirdan, N.A.M. Obaid. Preparation of New Azo Dye Derived of Pharmaceutical Substances (Procaine and Vitamin B6) and Theoretically Studied as a Carbon Steel Corrosion Inhibitor. *Instrumentation Mesure Metrologie* **2025**, 24 (3), 229–236.
17. H.A. Abdullmajed, I.A. Alasady, H.T. Obaid, G.A. Mirdan, N.A.M. Obaid. Preparation of New Azo Dye Derived of Pharmaceutical Substances (Procaine and Vitamin B6) and Theoretically Studied as a Carbon Steel Corrosion Inhibitor. *Instrumentation Mesure Metrologie* **2025**, 24 (3), 229–236.
18. Q.M.A. Hassan, R.H. Al-Asadi, H.A. Sultan, et al. A novel azo compound derived from ethyl-4-amino benzoate: synthesis, nonlinear optical properties and DFT investigations. *Optical and Quantum Electronics* **2023**, 55 (5).
19. Boudjellal, E.-H.E.-O. M., A.M. W.N.A. Impact de l'aluminium sur la santé humaine. *Algerian Journal of Nutrition and Food Sciences (AJNFS)* **2022**, 1 (03), 11–16.
20. R.K. Agarwal, V. Kumar. Studies on the effect of various anions and pyridine on the stereochemistry of lanthanide(III) coordination compounds of 4[N-(2'-hydroxy-1'-naphthalidene)amino] antipyrine thiosemicarbazone. *Phosphorus, Sulfur and Silicon and the Related Elements* **2010**, 185 (7), 1469–1483.
21. A. Smania, Jr., F.D. Monache, E. de F.A. Smania, R.S. Cuneo. Antibacterial Activity of Steroidal Compounds Isolated from *Ganoderma applanatum* (Pers.) Pat. (Aphyllporomycetidae) Fruit Body. *Int. J. Med. Mushr.* **1999**, 1 (4), 325–330.
22. Ü. Çakir, H. Temel, S. İlhan, H.I. Uğraş. Spectroscopic and Conductance Studies of New Transition Metal Complexes with a Schiff Base Derived from 4-Methoxybenzaldehyde and 1,2-bis(p-Aminophenoxy)ethane. *Spectroscopy Letters* **2003**, 36 (5–6), 429–440.
23. M.A. El-ghamry, K.M. Nassir, F.M. Elzawawi, A.A.A. Aziz, S.M. Abu-El-Wafa. Novel nanoparticle-size metal complexes derived from acyclovir. Spectroscopic characterization, thermal analysis, antitumor screening, and DNA cleavage, as well as 3D modeling, docking, and electrical conductivity studies. *J. Mol. Structure* **2021**, 1235, 130235.
24. K.J. Al-adilee, H.A.K. Kyhoiesh. Preparation and Identification of Some Metal Complexes with New Heterocyclic Azo Dye Ligand 2-[2'-(1-Hydroxy -4- Chloro phenyl) azo]- Imidazole and their Spectral and Thermal Studies. *J. Mol. Str.*, **2017**, 1137, 160-178.
25. K.N. Aziz, K.M. Ahmed, R.A. Omer, A.F. Qader, E.I. Abdulkareem. A review of coordination compounds: Structure, stability, and biological significance. *Reviews in Inorganic Chemistry* **2025**, 45 (1), 1–19.
26. M. Kato. Experimental Techniques; **2022**.
27. J. Liu, S.C. Lorraine, B.S. Dolinar, J.M. Hoover. Aerobic Oxidation Reactivity of Well-Defined Cobalt(II) and Cobalt(III) Aminophenol Complexes. *Inorganic Chemistry* **2022**, 61 (16), 6008–6016.
28. G.A. Bain, J.F. Berry. Diamagnetic corrections and Pascal's constants. *Journal of Chemical Education* **2008**, 85 (4), 532–536.
29. A.L. El-Ansary, N.S. Abdel-Kader. Synthesis, Characterization of La(III), Nd(III), and Er(III) Complexes with Schiff Bases Derived from Benzopyran-4-one and Thier Fluorescence Study. *International J. Inorganic Chemistry* **2012**, 2012 (1), 1–13.
30. C.R. Bhattacharjee, P. Goswami, P. Mondal. Synthesis, reactivity, thermal, electrochemical and magnetic studies on iron(III) complexes of tetradentate Schiff base ligands. *Inorganica Chimica Acta* **2012**, 387, 86–92.
31. S. Gordon, B.J. McBride. Computer program for calculation of complex chemical equilibrium compositions rocket performance incident and reflected shocks, and Chapman-Jouguet detonations. *NASA Report SP-273, Interim Revision* **1976**.
32. M.A. Brown, A. Paulenova, A. V. Gelis. Aqueous complexation of thorium(IV), uranium(IV), neptunium(IV), plutonium(III/IV), and cerium(III/IV) with DTPA. *Inorganic Chemistry* **2012**, 51 (14), 7741–7748.
33. S.V.C. De Souza, R.G. Junqueira. A procedure to assess linearity by ordinary least squares method. *Analytica Chimica Acta* **2005**, 552 (1–2), 25–35.